DTU Library

Effect of strain on surface diffusion and nucleation

Brune, Harald; Bromann, Karsten; Röder, Holger; Kern, Klaus; Jacobsen, Joachim; Stoltze, Per; Jacobsen, Karsten Wedel; Nørskov, Jens Kehlet

[Link back to DTU Orbit]

Effect of strain on surface diffusion and nucleation

Harald Brune, Karsten Bromann, Holger Röder, and Klaus Kern
Institut de Physique Expérimentale, Ecole Polytechnique Féderalé de Lausanne, CH-1015 Lausanne, Switzerland

Joachim Jacobsen, Per Stoltze, Karsten Jacobsen, and Jens Nørskov
Center for Atomic-Scale Materials Physics and Physics Department, Technical University of Denmark, DK-2800 Lyngby, Denmark
(Received 5 September 1995)

The influence of strain on diffusion and nucleation has been studied by means of scanning tunneling microscopy and effective-medium theory for Ag self-diffusion on strained and unstrained (111) surfaces. Experimentally, the diffusion barrier is observed to be substantially lower on a pseudomorphic Ag monolayer on Pt(111), 60 meV, compared to that on Ag(111), 97 meV. The calculations show that this strong effect is due to the 4.2% compressive strain of the Ag monolayer on Pt. It is shown that in general isotropic two-dimensional strain as well as its relief via dislocations have a drastic effect on surface diffusion and nucleation in heteroepitaxy and are thus of significance for the film morphology in the kinetic growth regime.

It is well established that the strain resulting from lattice mismatch in heteroepitaxy can have a strong impact on the film morphology for thermodynamic reasons. The increase in strain energy with increasing film thickness often induces an instability in growth mode where two-dimensional (2D) growth is succeeded by three-dimensional growth above a critical thickness.[1] As a second effect the strain energy in general causes a pseudomorphic film at a certain thickness to change to disregistry, where part of the strain is relieved by the introduction of misfit dislocations (see, e.g., Refs. 2 and 3).

In most cases thin films are grown far from equilibrium, hence their morphology is governed by kinetics rather than by thermodynamics. In the kinetic growth regime 3D growth results if nucleation and island growth on top of existing islands sets in prior to coalescence of these islands. This is determined, first, by the mean free path of a diffusing adatom on top of islands with respect to their size and form, i.e., whether and how often it visits the island edge, and second, by the rate for the adatom to descend the edge with respect to its visiting rate. In homoepitaxy, if no reconstruction is involved, these quantities are independent of layer thickness. Therefore, the mean free path on top of an island and on the terrace below are identical. The latter determines the distance between islands and thus their maximum size before coalescence. Thus the islands grow never bigger than the mean free path of an adatom on top of them. Hence in homoepitaxy each adatom can reach the descending edge at least once and, therefore, it is solely the activation barrier to descend the edge that determines the morphology, whereas surface diffusion is less important.

In heteroepitaxy, as we will demonstrate in the present paper, this is in general quite different. Here, due to the inherent strain, surface diffusion can strongly alter from layer to layer and thus play the dominant role in determining the film morphology. Strain, if isotropic, is simply a variation of the in-plane lattice constant. It is shown that surface diffusion is rather sensitive to that parameter. If strain is anisotropic, i.e., if dislocations have formed, this is found to have a strong impact on adatom mobilities as well.

Our scanning tunneling microscopy (STM) study of surface diffusion on strained Ag layers grown on Pt(111) reveals a drastic layer dependence of adatom mobilities manifested in layer-dependent island densities. The first Ag layer grows pseudomorphically; it is thus under an isotropic compressive strain of 4.2%.[3] This leads to a decrease of the Ag surface diffusion barrier to only 60 meV, compared to 97 meV measured for self-diffusion on unstrained Ag(111). While an influence of strain on diffusion had been proposed some years ago in a theoretical study of Ga on GaAs(001),[4] there was no direct experimental evidence of this important effect. Calculations with effective-medium theory (EMT) demonstrate that the decrease of the diffusion barrier on the pseudomorphic Ag monolayer is indeed due to strain; the electronic coupling from the substrate even weakens the effect. The calculations indicate that, in general, surface diffusion depends rather sensitively on compressive or tensile strain. Computations for a laterally strained Ag(111) slab show that at moderate variations of the lattice parameter ($\pm2\%$) the diffusion barrier scales nearly linearly with the nearest-neighbor distance, decreasing with compressive strain and increasing with tensile strain. This can be understood in an intuitive way. Lattice compression moves the adatom out so that it experiences a less corrugated potential energy surface, while expansion has the inverse effect.

The experiments were performed with a variable-temperature STM (25–800 K) operating in ultrahigh vacuum.[5] The Ag films on Pt(111) are prepared by deposition of Ag at 450 K and subsequent annealing to 800 K. The first monolayer grows pseudomorphically, while the higher layers (2–3 ML) relax via the formation of periodic arrays of dislocations that transform into weakly modulated incommensurate films at larger thickness (4–20 ML).[3,6,7] Very thick films (>40 ML) show no modulation and have the Ag(111) interplanar lattice constant and symmetry as characterized by He diffraction.[6] STM images revealed that both the pseudomorphic Ag layer on Pt(111) and the Ag(111) surface consisted of extended flat terraces that were free of dislocations. For the study of nucleation kinetics, submonolayer coverages have been deposited (flux 1.1×10^{-3} ML/s) subsequently

a)   b)   c)   d)
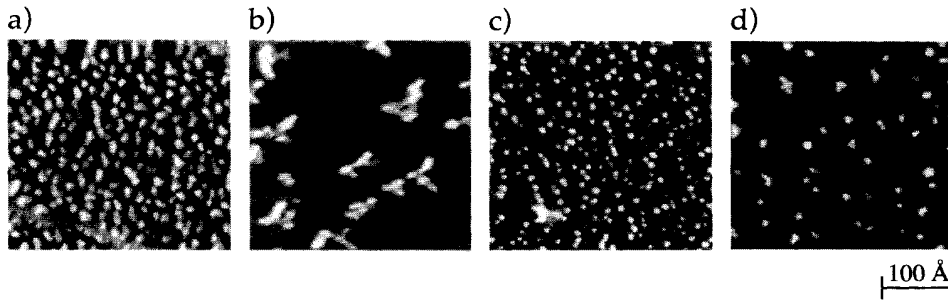

$\vdash\!\!100\ \text{Å}\!\!\dashv$

FIG. 1. STM images showing the nucleation of submonolayer coverages of Ag on Pt(111) (a), 1 ML Ag/Pt(111) (b), 2 ML Ag/Pt(111) (c), and Ag(111) (d), respectively [(a) saturation island density $N_x = 1.7 \times 10^{-2}$ islands per Pt(111) surface atoms, $\Theta = 0.12$ ML; (b) $N_x = 6.6 \times 10^{-4}$, $\Theta = 0.05$ ML; (c) $N = 1.6 \times 10^{-2}$, $\Theta = 0.03$ ML (note that the mean island size Θ/N is 2, i.e., saturation is not yet reached for this case); (d) $N_x = 3.8 \times 10^{-3}$, $\Theta = 0.03$ ML; (a) and (b) $T = 65$ K; (c) and (d), $T = 60$ K; for all images, deposition flux $R = 1.1 \times 10^{-3}$ ML s^{-1}, size 307×307 Å^2]. All STM images are taken isotherm to deposition.

onto these layers at various temperatures. Island densities are given in islands per Pt substrate atom, i.e., in ML. They were obtained on extended terraces and corrected for lateral drift.[8]

The strong layer dependence of nucleation kinetics becomes evident from inspection of Fig. 1. It shows nucleation on the substrate (a), the first (b), and second (c) Ag layer, as well as on a 50-ML-thick Ag layer that has adopted Ag(111) geometry (d). We will now briefly describe the concept of relating island densities to diffusion.[9] In all four cases nucleation of islands takes place at the time of deposition. The resulting island density is stationary under isothermal conditions where it is imaged after deposition. At the beginning of deposition the density of nuclei steadily increases as a function of coverage (nucleation regime) until it becomes more probable that diffusing atoms attach to existing islands rather than create new ones. In this growth regime the island density stays nearly constant in a wide coverage range of $\Theta = 0.05$–0.20 ML, until it eventually decreases due to coalescence. Its maximum, the saturation island density, is determined by the ratio of the diffusivity to the deposition flux and therefore a measure for the adatom mobility. Except for Fig. 1(c) all images in Fig. 1 show the surface after an island density close to saturation has formed; thus the mean island distance can be regarded as an estimate for the mean free path of a diffusing adatom.

The island density shows an oscillatory behavior with layer thickness. It decreases by a factor of 26 when going from the Pt substrate to the pseudomorphic first layer. The density then attains again the substrate value on the second layer. In this discommensurate layer the strain is relieved in a trigonal dislocation network which becomes visible as dark lines that include small triangles where they cross each other.[3] [Note that in Fig. 1(c) the island density is not yet at saturation, which implies an even higher saturation density, i.e., lower mobility than suggested from the figure.] Nucleation on Ag(111) again leads to a slight decrease in island density [see Fig. 1(d)]. Already from this set of STM images, which was depicted at 60–65 K, it can be concluded that there is a strong influence of layer thickness on the adatom mobilities. However, care has to be taken when drawing conclusions on kinetic parameters from experimental data for a single temperature. As will be shown below, the strong layer-dependent effect, manifest in Fig. 1, can even be reversed when going to higher temperatures.

In order to get quantitative insight into the diffusion and nucleation of Ag on these layers, we have measured the saturation island density as a function of temperature for the three cases of an isotropic substrate. The result is shown in the Arrhenius representation in Fig. 2. For Ag on Pt(111) it has been demonstrated recently that application of mean-field nucleation theory[10] yields reliable information on the energy barrier and prefactor for surface diffusion $(E_m = 157 \pm 10$ meV, $\nu_0 = 1 \times 10^{13 \pm 0.4}$ s$^{-1})$.[9] With these values the experimental island densities are exactly reproduced for all temperatures investigated, either upon integration of rate equations,[9] or by kinetic Monte Carlo simulations with these parameters (we applied the same Monte Carlo code as in Ref. 11). This gives us confidence in applying the same procedure also to the two other cases, i.e., Ag/1 ML Ag/ Pt(111) and Ag/Ag(111). They equally show an Arrhenius behavior on the saturation island density (see Fig. 2). A prerequisite for adequate application of nucleation theory is the knowledge of the critical cluster size (i), and, respectively, that of a stable cluster $(i+1)$. (Clusters of size $\leq i$ are unstable with respect to dissociation on the time scale of deposition.) Annealing experiments as well as the absence of sharp bends in $\log_{10} N_x$ versus $(1/T)$ plots[9] show that dimers are stable (and immobile), i.e., $i = 1$, in all three cases for the temperatures for which island densities are shown in Fig. 2. In this case the terrace diffusion can be directly deduced
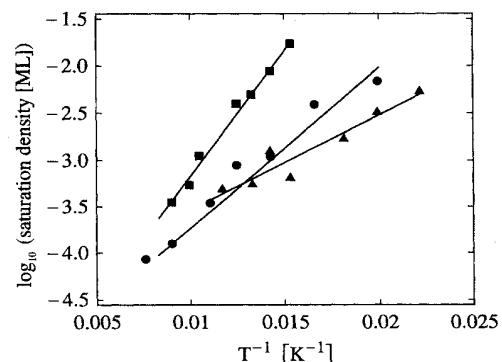

FIG. 2. Arrhenius plot of saturation island densities derived from STM for nucleation of Ag on Pt(111) (■), on 1 ML Ag adsorbed on Pt(111) (▲), and on Ag(111) (●), respectively.

TABLE I. Barriers for Ag surface diffusion as function of Ag layer thickness on Pt(111) as obtained from STM compared to calculations with EMT (s denotes compressive strain).

	E_m (meV) STM	E_m (meV) EMT	E_b (eV) EMT
Ag/Pt(111)	157 ± 10	80	2.529
Ag/1 ML Ag/Pt(111)	60 ± 10	50	2.374
Ag/Ag(111)	97 ± 10	67	2.400
Ag/Ag(111) $s = 4.2\%$		41	2.380

from the Arrhenius plot of saturation island densities without knowledge of dissociation energies.[10]

For Ag diffusion on the isotropically strained first layer on Pt(111) we find $E_m = 60 \pm 10$ meV and from the intersection of the line fit with the ordinate $\nu_0 = 1 \times 10^{9 \pm 0.6}$ s^{-1}. Compared to the substrate this is a rather low barrier, which explains the drastic decrease in island density at 65 K evident from Fig. 1(b). For Ag self-diffusion on Ag(111) we obtain $E_m = 97 \pm 10$ meV for the diffusion barrier with the corresponding attempt frequency $\nu_0 = 2 \times 10^{11 \pm 0.5}$ s^{-1}.[12] Therefore at low T the island density on the thick Ag(111) layer is in between that on the first layer and on the Pt substrate [see Fig. 1(d)]. In the presence of dislocations [Fig. 1(c)], on the other hand, the island density is higher than on unstrained Ag(111), which means that a network of dislocations can confine diffusing adatoms and thereby strongly increase the island density, as discussed in more detail below. Note that with the barriers, also, a change in prefactor can go hand in hand. From Fig. 2 it is seen that this leads to crossing at $T = 85$ K. From this temperature on, the ratio of island densities of the strained and unstrained case is inverted.

The most conspicuous and probably unexpected effect uncovered by the STM experiment is the low barrier for Ag diffusion on the pseudomorphic Ag layer compared to unstrained Ag(111). Two effects are conceivable to cause the observed lowering. It may either be due to the 4.2% compressive strain or an effect of the electronic adlayer-substrate coupling. In order to decide which is dominant we performed EMT calculations.[13,14] For this purpose we considered a Ag atom adsorbed on a 6×6 cell of a five-layer slab. The three upper layers are free to relax. The adatom is pulled over this surface, allowing its position to relax freely in a plane perpendicular to the vector of displacement, in order to find the minimum of total energy in the course of the displacement. The diffusion barrier E_m is then determined as the difference in total energy between the transition state (bridge site) and the preferred adsorption site (fcc hollow).

The results of this calculation are summarized in comparison with experiment in Table I. Regarding absolute values, it is seen that the EMT underestimates diffusion barriers, which is well known from other systems as, e.g., for Pt/Pt(111).[11] However, the order of diffusion barriers is in accordance with experiment; the barrier is highest for Ag/Pt (80 meV), lower for Ag self-diffusion (67 meV), and substantially decreased for diffusion on the first pseudomorphic layer (50 meV). In order to distinguish between the effect of strain and the presence of the substrate we calculated Ag diffusion on a Ag(111) slab that is under 4.2% compressive strain. (This has been achieved by reducing the lateral dimensions of the
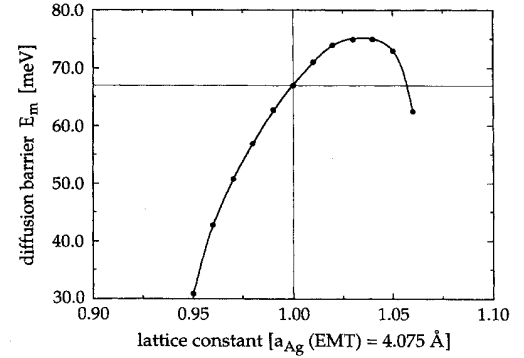

FIG. 3. Barrier for Ag self-diffusion on a Ag(111) slab as a function of tensile or compressive strain as calculated with EMT.

slab by 4.2% compared to the EMT equilibrium value for Ag; as above, the three uppermost layers were free to relax.) The result is that in the absence of electronic Ag-Pt coupling the effect is even more pronounced; the barrier is lowered to 41 meV. We can thus safely conclude that strain is the reason for the decrease in diffusion barrier on the first Ag layer, which is compressed into registry with the Pt(111) substrate.

The general sensitivity of surface diffusion on compressive and tensile stain is illustrated in Fig. 3. It shows Ag diffusion barriers on differently strained Ag(111) slabs, again calculated with EMT. A small strain of $\pm 2\%$ affects the diffusion barrier almost linearly; for tensile strain it is increased, for compressive strain decreased. The barrier has its maximum of 75 meV at 3.5% tensile strain. It drops upon further increase of the lattice constant. For compressive strain, migration becomes increasingly fast; the barrier attains half of the unstrained value at 4.8% compression. Looking at the binding energies for the adsorbed Ag atoms (E_b), listed in Table I, we estimate that the decrease of diffusion barrier due to compressive strain is mainly caused by a smaller binding energy in the hollow site. As expected, for tensile strain the binding energy in the hollow is increased, which leads to the increase in E_m. At high tensile strain ($>3.5\%$) the transition state drastically decreases its energy, which explains the bending of the curve and the second decrease in E_m. This can be understood by the increasing softness of the layer with increasing lattice constant. Thus atoms in the bridge configuration, which corresponds to the transition state, can relax more efficiently.

For nucleation of Ag on a regular array of dislocations, we have seen in Fig. 1(c) that the island density is strongly increased with respect to the unstrained and the homogeneously strained case. Further, we find that only a few of the nuclei form directly on dislocations. For increasing temperature, nucleation substantially differs from that on isotropic surfaces. The island density asymptotically approaches a minimum at 110 K, where one island forms per unit cell of the dislocation network. Figures 4(a) and 4(b) show nucleation at 90 and 110 K with an average of 1.3 and 1.1 islands per superstructure unit cell. Note that, again, only very few of the islands form on dislocations. The majority sit on the hexagons of the unit cell, which are pseudomorphic with fcc stacking.[3,7] From this we conclude that the dislocations constitute a rather effective repulsive barrier for adatoms to
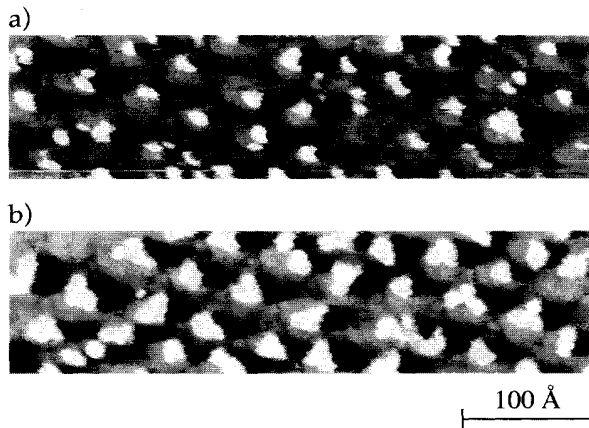
a)

b)

|← 100 Å →|

FIG. 4. STM images showing the influence of dislocations on nucleation of Ag on 2 ML Ag/Pt(111). (a) $T=90$ K, $N_x=1.3$ per unit cell of superstructure, $\Theta=0.03$ ML; and (b) $T=110$ K, $N_x=1.1$ per unit cell of superstructure, $\Theta=0.12$ ML (image size 450×120 Å^2).

cross, which confines them to the pseudomorphic domains. At higher temperatures this confinement artificially increases the island density even if diffusion on the homogeneously strained parts of the surface may be fast. A similar effect has recently been observed for Ni nucleation on the dislocation network of Ni on Ru(0001).[15]

This shows that the influence of dislocations on diffusion and nucleation is substantial; in our particular case they are repulsive, even though they have a lower density and thus an increased diffusion barrier. There are a variety of possible ways for dislocations to influence diffusion and nucleation. It has been shown for Ni, Fe, and Co on Au(111) (Ref. 16) that the elbows of the herringbone reconstruction can act as traps. In contrast, recent results for Al on this surface indicate that this is not the general rule.[17] Whether a dislocation acts as sink or repulsive wall for diffusing adatoms depends on both the binding energy and the diffusion barrier when crossing the dislocation and has to be investigated for the particular case. For Pt/Pt(111), e.g., the barrier between adjacent fcc sites basically stays constant whereas the total energy in-

creases upon crossing a dislocation.[18] Even if the change in total energy is small it is feasible to lead to drastic changes in diffusivity because atoms have to make several successive jumps in unfavorable directions to overcome a dislocation. No matter how dislocations affect diffusion and thereby nucleation, there is no question as to their strong influence, as it has been observed, to our knowledge, in every case investigated so far.

While we have demonstrated the impact of misfit strain on surface diffusion and nucleation for a particular model system, its implications for heteroepitaxial growth in the kinetic regime are of general significance. It is generally true that the adatom mobility on an isotropically strained layer will be modified relative to the strain-free surface. To the extent that the kinetics is simply dominated by strain effects,[19] this work indicates that compressive strain will decrease and tensile strain will increase diffusion barriers. Modified adatom mobilities and thus altered nucleation densities on successive layers due to strain can substantially affect the growth morphology. An enhanced adatom mobility on top of a certain layer, in general, promotes its smoother growth while the inverse effect will drive the system towards rough three-dimensional growth. These effects might be used to shape the growth mode of a heteroepitaxial system on pure kinetic grounds. The nucleation rate is also critically influenced through strain-induced formation of a dislocation network. These dislocations can act as heterogeneous nucleation centers or as repulsive barriers. Their influence is not limited to heteroepitaxy. Even in homoepitaxy, for surfaces that have intrinsic tensile stress and thus reconstruct, the presence of dislocations can influence the growth morphology. For Pt/Pt(111) the large increase of the nucleation rate due to the dislocation confinement is thought to give rise to an anomalous, perfect 2D growth at 650 K.[20] More than 150 undamped oscillations are seen in the specular He intensity, where a much faster decay of oscillations was expected without the reconstruction. The concept of layer-dependent adatom mobilities and island densities caused by strain seems to be of general validity and constitutes, in addition to the barrier for interlayer diffusion, an essential ingredient for the kinetic modeling of film growth.

[1] J. H. v. d. Merwe et al., Surf. Sci. 312, 387 (1994).

[2] C. Günther et al., Phys. Rev. Lett. 74, 754 (1995).

[3] H. Brune et al., Phys. Rev. B 49, 2997 (1994).

[4] S. V. Ghaisas, Surf. Sci. 223, 441 (1989); see also H. Spjut et al., Surf. Sci. 306, 233 (1994); C. Roland et al., Phys. Rev. B 46, 13 428 (1992).

[5] H. Brune et al., Appl. Phys. A 60, 167 (1995).

[6] C. Romainczyk, M. Krzykowski, P. Zeppenfeld, G. Comsa, and K. Kern (unpublished).

[7] G. Rangelov et al., Surf. Sci. 331-333, 948 (1995).

[8] The scanned area can vary (up to ±30%) due to lateral drift in the slow scan direction. For determination of the island densities this has been accounted for by considering the drift vectors of consecutive images.

[9] H. Brune et al., Phys. Rev. Lett. 73, 1995 (1994).

[10] J. A. Venables et al., Rep. Prog. Phys. 47, 399 (1984).

[11] J. Jacobsen et al., Phys. Rev. Lett. 74, 2295 (1995).

[12] The error for E_m is predominantly due to scatter of the data. That, for ν_0, comes from the uncertainty of $\eta(\Theta)$ in Eq. (2.15) of Ref. 10 [we assumed $\eta(\Theta_{saturation})=0.20\pm0.04$, see Fig. 6(c) for $i=1$ in that reference] and by the error in slope, i.e., in E_m.

[13] K. W. Jacobsen et al., Phys. Rev. B 35, 7423 (1987).

[14] P. Stoltze, J. Phys. Condens. Matter 6, 9495 (1994).

[15] J. A. Meyer et al., Phys. Rev. Lett. 74, 3864 (1995).

[16] D. D. Chambliss et al., J. Magn. Magn. Mater. 121, 1 (1993).

[17] B. Fischer, L. Nedelmann, A. Fricke, H. Brune, and K. Kern (unpublished).

[18] J. Jacobsen et al., Surf. Sci. 317, 8 (1994).

[19] Without detailed calculations, such as those presented here, it is not possible to predict with confidence if a given system is dominated by strain or by electronic coupling.

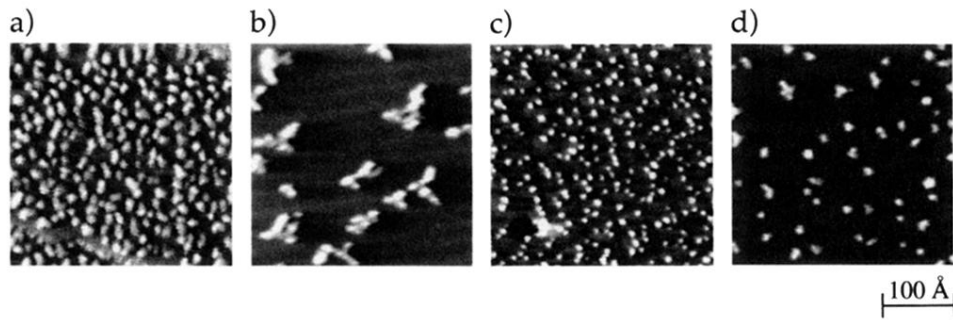[20] T. Michely, M. Hohage, S. Esch, and G. Cosma (unpublished).

FIG. 1. STM images showing the nucleation of submonolayer coverages of Ag on Pt(111) (a), 1 ML Ag/Pt(111) (b), 2 ML Ag/Pt(111) (c), and Ag(111) (d), respectively [(a) saturation island density $N_x = 1.7 \times 10^{-2}$ islands per Pt(111) surface atoms, $\Theta = 0.12$ ML; (b) $N_x = 6.6 \times 10^{-4}$, $\Theta = 0.05$ ML; (c) $N = 1.6 \times 10^{-2}$, $\Theta = 0.03$ ML (note that the mean island size Θ/N is 2, i.e., saturation is not yet reached for this case); (d) $N_x = 3.8 \times 10^{-3}$, $\Theta = 0.03$ ML; (a) and (b) $T = 65$ K; (c) and (d), $T = 60$ K; for all images, deposition flux $R = 1.1 \times 10^{-3}$ ML s^{-1}, size 307×307 Å^2]. All STM images are taken isotherm to deposition.
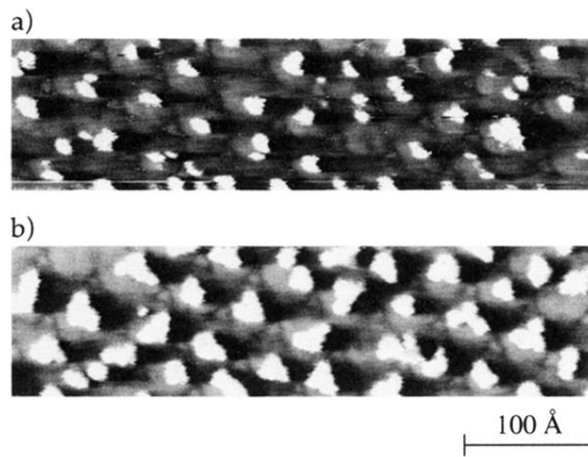
FIG. 4. STM images showing the influence of dislocations on nucleation of Ag on 2 ML Ag/Pt(111). (a) $T=90$ K, $N_x=1.3$ per unit cell of superstructure, $\Theta=0.03$ ML; and (b) $T=110$ K, $N_x=1.1$ per unit cell of superstructure, $\Theta=0.12$ ML (image size 450×120 Å^2).